Journal of Computational and Applied Mathematics 233 (2010) 3167–3177

Contents lists available at ScienceDirect

Journal of Computational and Applied Mathematics

journal homepage: www.elsevier.com/locate/cam

An adaptive time discretization of the classical and the dual porosity model of Richards' equation

Michal Kuráž [a,*], Petr Mayer [b], Matěj Lepš [c], Dagmar Trpkošová [d]

[a] Czech University of Life Sciences Prague, Faculty of Environmental Sciences, Department of Water Resources and Environmental Modeling, Czech Republic
[b] Czech Technical University in Prague, Faculty of Civil Engineering, Department of Mathematics, Czech Republic
[c] Czech Technical University in Prague, Faculty of Civil Engineering, Department of Mechanics, Czech Republic
[d] Charles University in Prague, Faculty of Science, Institute of Hydrogeology, Engineering Geology and Applied Geophysics, Czech Republic

ARTICLE INFO

Article history:
Received 14 April 2009
Received in revised form 11 September 2009

Keywords:
Darcy's law
Variable saturation
Retention curve
Mass balance
Adaptive time discretization
Preferential flow
Homogenization
Parameter identification
Multi-objective evolutionary algorithm

ABSTRACT

This paper presents a numerical solution to the equations describing Darcian flow in a variably saturated porous medium—a classical Richards' equation model Richards (1931) [1] and an extension of it that approximates the flow in media with preferential paths—a dual porosity model Gerke and van Genuchten (1993) [8]. A numerical solver to this problem, the DRUtES computer program, was developed and released during our investigation. A new technique which maintains an adaptive time step, defined here as the Retention Curve Zone Approach, was constructed and tested. The aim was to limit the error of a linear approximation to the time derivative part. Finally, parameter identification was performed in order to compare the behavior of the dual porosity model with data obtained from a non-homogenized fracture and matrix flow simulation experiment.

1. Introduction

The problem of predicting the fluid movement in an unsaturated/saturated zone is important in many fields, ranging from agricultural via hydrology to technical applications of dangerous waste disposal in deep rock formations.

The mathematical model of unsaturated flow was originally published in [1]. This formula, usually identified as the mixed form of Richards' equation, states that

$$\frac{\partial \theta}{\partial t} - \nabla.\,(K(\theta)\nabla h) - \frac{\partial K(h)}{\partial z} = 0 \tag{1}$$

where θ is the water content of a porous material [–], h is the pressure head [L], $K(\theta)$ is the unsaturated hydraulic conductivity function [$L.T^{-1}$], z denotes the vertical dimension [L], assumed positive upwards, and the porous medium is assumed to be isotropic. Appropriate constitutive relationships between θ and h, K and h, are also assumed.

This PDE can be generalized as a quasilinear elliptic–parabolic differential equation and as a degenerate convection–diffusion problem. A proof of the existence of a solution is given in [2]. A technique for an accurate numerical solution is published in [3]. One of the recent outstanding work presenting a numerical method based on a relaxation scheme to the time derivative term and method of characteristics to the convection term is published in [4,5].

* Corresponding address: Czech University of Life Sciences Prague, Faculty of Environmental Sciences, Department of Water Resources and Environmental Modeling, Kamycka 129, 16521 Praha 6 - Suchdol, Czech Republic.
E-mail address: michal.kuraz@fsv.cvut.cz (M. Kuráž).

0377-0427/$ – see front matter © 2009 Elsevier B.V. All rights reserved.
doi:10.1016/j.cam.2009.11.056

In many practical engineering problems it is necessary to deal with an environment that cannot be accurately homogenized by a single set of porous environment parameters, due to systems of fractures and fissures. In order to improve the approximation, dual porosity models have been extended and used. A conceptual double continua approach for fissured groundwater systems was first introduced as early as 1960, in [6,7]. In order to simulate the preferential flow of water under variably saturated conditions, a set of coupled Richards' equations describing the transient water flow in each of two subsystems was suggested in [8]. A different approach was recently published in [9], where the flow domain representing the fractures is described by a kinematic wave equation, using a method based on [10].

A numerical technique for maintaining the coupled system of Richards' equations was originally handled in [8]. A recommended approach based on a coupled solution produces matrices that are twice as large as the classical Richards model and have some extra bands depending on a problem dimension. A domain decomposition technique for lowering the computational effort is presented in [11]. The resulting algebraic system was subsequently partitioned in the time domain with a staggered implicit–implicit partitioning scheme. The partition integration procedures were carried out sequentially for the two subsystems, and coupled by temporal extrapolation techniques. Unfortunately for certain applications this method may suffer from a numerical stability restriction [11].

When the fissure and fracture system is homogenized to a porous environment, an important task is to identify the parameters of its unsaturated hydraulic properties. The suitability of direct gradient methods for identifying the unsaturated hydraulic parameters based on measurements is discussed in [12]. Generally speaking, in certain ranges, identification of the unsaturated hydraulic parameters might be a non-convex problem with local extremes. Direct mathematical methods have not yet been satisfactory solved in this field. In general, some stochastic approaches based on genetic algorithms might bring desirable results. The application of genetic algorithms for identifying hydraulic unsaturated parameters has been discussed in [13].

The goal of this paper is to demonstrate a numerical solution of a model describing the potential flow in a variably saturated porous medium. This work consist of the two main parts. In the first part (sections between 2 and the Section 3.4) a classical model of Richards' equation is retained together with a new technique maintaining an adaptive time step, defined here as the Retention Curve Zone Approach. The aim was to limit the error of a linear approximation to the time derivative part. The second part of this paper (Sections from 4 to the Section 5.3) discuss its extension—the dual porosity model. Its numerical solution was based on results discussed in Section 3.4—the case study of the classical Richards' equation model. The dual porosity model evaluation in Section 5.1 is based on calibrating to the data obtained from the numerical simulation on a sample with discrete fractures.

2. Mathematical model of the single domain problem—a classical Richards equation model

This section presents the mathematical model commonly used to describe Darcian flow in a variably saturated porous media—the classical Richards' equation. This approach is suitable for flow environments without any significant preferential flow paths like fissures, fractures, etc. Unsaturated porous material properties were already described by a variety of empirical laws, formulas, which can be attached to the original Richards' equation from [1].

2.1. Governing equations

Darcy's approach to groundwater flow is basically applicable for both the saturated and the unsaturated flow (moisture movement), and considers the flow as diffusion. By an application of the unsaturated Darcy's flow law to the mass conservation law Richards' equation is obtained [14]. Three standard forms of Richards' equation are identified—*mixed*, h-based and θ-based forms. In the mixed form, which was originally published in [1], see (1), both the pressure head and the water content are the primary solved variable. In the 'h-based' form

$$C(h)\frac{\partial h}{\partial t} - \nabla.(K(h)\nabla h) - \frac{\partial K(h)}{\partial z} = 0 \tag{2}$$

where $C(h) = \frac{\mathrm{d}\theta}{\mathrm{d}h}$, is the specific water capacity function $[L^{-1}]$, the pressure head is the primary solved variable. In the 'θ-based' form

$$\frac{\partial \theta}{\partial t} - \nabla.(D(\theta)\nabla\theta) - \frac{\partial K(\theta)}{\partial z} = 0 \tag{3}$$

where $D(\theta) = \frac{K(\theta)}{C(\theta)}$, is unsaturated diffusivity $[L^2.T^{-1}]$ and the water content is the primary solved variable.

Eqs. (1) and (2) are defined for $\theta \in (\theta_r, \theta_s\rangle$ and $h \in (-\infty, +\infty)$. θ_r and θ_s are the water content limits of the unsaturated flow. Eq. (3) is defined only for the unsaturated flow, and thus $\theta \in (\theta_r, \theta_s\rangle$. When applying the constitutive relation between θ and h this equation solves only negative heads. This limits some technical applications, e.g. a positive pressure head as a boundary condition.

2.1.1. Constitutive relations—unsaturated hydraulic material properties

The solution to Richards' equation is based on knowledge of the relation between the pore pressure head and the water content, the water content and the unsaturated hydraulic conductivity. The relation between saturation and unsaturated

hydraulic conductivity is based on [15]

$$K_r(h) = \sqrt{\left(\frac{\theta}{\theta_s}\right)}\left(\frac{\int_{\theta_r}^{\theta}\frac{1}{h(\theta)}\mathrm{d}\theta}{\int_{\theta_r}^{\theta_S}\frac{1}{h(\theta)}\mathrm{d}\theta}\right)^2 \tag{4}$$

where $K_r(h)$ is the relative hydraulic conductivity [−], and where $K_r = \frac{K(h)}{K_s}$, where K_s is the saturated hydraulic conductivity $[L.T^{-1}]$.

An analytical formula (van Genuchten's equation) describing the relation between saturation—mass and pore suction was derived in [16]

$$\theta(h) = \begin{cases} \dfrac{\theta_s - \theta_r}{(\theta_S + (-\alpha h)^n)^m} + \theta_r, & \text{if } h \in (-\infty, 0) \\ \theta_S, & \text{if } h \in \langle 0, +\infty) \end{cases} \tag{5}$$

where θ_s is the saturation water content equal to porosity [−], θ_r is the residual water content [−], α $[L^{-1}]$, n [−], m [−] are empirical porous environment variables, dependent on pore size distribution and shapes, θ is the actual saturation [−], h is the pressure head $[L]$, negative for unsaturated conditions.

An analytical formula to (4) was derived in [17] with restriction to m coefficient ($m = 1 - \frac{1}{n}$), but a standard numerical integration techniques, e.g. the Gauss quadrature formula, gives satisfactory results without any parameter restrictions.

3. Numerical solution of the classical Richards' equation model

A numerical solution to (1) and (2) is presented in this section. Although Eq. (3) offers outstanding mass balance behavior it will not be further discussed here, due to its limits in its definition scope to negative pressure heads.

Due to a nonlinear nature of the functions (5) and (4) a special technique to maintain an adaptive time discretization should be considered.

3.1. Numerical solution of the mixed-form equation

This numerical solution is fully based on [3]. A technique known as Modified Picard Iteration was defined by Celia's work as follows

$$\left(\frac{1}{\Delta t}C^{n+1,m}\right)\delta^m - \nabla.\left(K(h)^{n+1,m}\nabla\delta^m\right) = \nabla.\left(K(h)^{n+1,m}\nabla h^{n+1,m}\right) + \frac{\partial K(h)^{n+1,m}}{\partial z} - \frac{\theta^{n+1,m} - \theta^{n,m}}{\Delta t} \tag{6}$$

where $\delta^m = h^{n+1,m} - h^{n,m}$, n denotes the actual iteration level and m denotes the node number. The variables of pressure and mass are both directly solved, and therefore perfect mass conservation is obtained. Eq. (2) was used as a predictor and (6) was the solution corrector.

The time derivative term was solved by the fully implicit Euler method, and the spatial derivative was solved by Galerkin's finite element method.

The adaptive time step is based on iteration criterion. The maximal number of iterations per time step is 20. If this number is exceeded solution is rejected and time step is decreased. If the amount of iterations is between 7 and 20, solution is accepted, but time step is unchanged, if it is bellow seven, solution is accepted and time step is increased.

3.2. Numerical solution of the h-based form equation

This solution was partly designed in a non-recommended way in [3]—the time derivative term was solved by the standard fully implicit Euler method, and the spatial derivative was solved by Galerkin's finite element method.

The further recommendation from [3] was fulfilled. The classical finite element approximation of (2) might suffer from oscillatory solutions. Such oscillations are not present in any finite difference solutions, which is explained by the difference in the treatment of the time derivative term. This implies that the diagonalized capacity matrices are to be preferred. This problem was already treated in [18] for the heat conduction equation, with the recommendation to diagonalize the capacity matrix.

The solver to (2) was constructed with a diagonalized capacity matrix as recommended in both [3,18].

The nonlinear coefficients $K(h)$ and $C(h)$ were calculated from the values of function h averaged over a particular time step.

According to [3], an error in the solution of (2) occurs due to the following approximation

$$\frac{\partial\theta(h)}{\partial t} = C(h)\frac{\partial h}{\partial t} \tag{7}$$

where, as mentioned above, $C(h) = \frac{\mathrm{d}\theta}{\mathrm{d}x}$ is the retention water capacity $[L^{-1}]$.

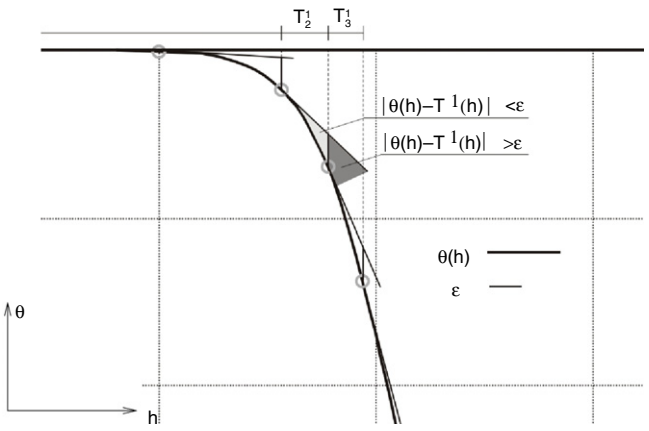

Fig. 1. The retention curve is divided into zones with a selected maximal value of the error of the first-order Taylor series.

Eq. (7) is valid in its differential form, but not in its discrete analogues, which states as follows

$$\frac{\Delta\theta(h)}{\Delta t} \approx C(h)\frac{\Delta h}{\Delta t}. \tag{8}$$

This inequality in the discrete form is amplified by the highly nonlinear nature of the specific water capacity term $C(h)$. This leads to significant mass balance errors in the h-based formulations, because the change of mass is calculated using discrete values $\frac{d\theta}{dt}$ while the approximation equations use the expansion $C(h)\frac{dh}{dt}$ [3].

An algorithm defined as the Retention Curve Zone Approach was designed to control an approximation error of (8) by maintenance of the adaptive time step.

3.2.1. Retention Curve Zone Approach

The Retention Curve Zone Approach is based on the assumption that even if the error of (8) cannot be prevented, it is possible to limit its value over the retention curve, and thus over the range of the mass balance changes in the material. Starting with a zero pressure head value, a first-order Taylor series to the retention curve is constructed. An error function of this approximation to the real retention curve is formulated. The bisection method is used to identify a point where this approximation exceeds the value of the user-defined maximal deviation (an error of this linear approximation, recommended approx. 10^{-5}). This point is used as the starting position for the next evaluation. Each point is stored in an array and acts as a border of the zones.

Fig. 1 and the following formula describes the procedure

$$h_{border,n} : |\theta(h_{border,n}) - T^1_{h_{border,n-1}}(h_{border,n})| - \varepsilon = 0$$

where $\theta(h)$ is the retention curve function, $T^1_{h_{border,n-1}}$ is the first-order Taylor series constructed as a tangent to the retention curve in the previous point, $h_{border,n}$ is a recent zone border—the unknown value to be numerically identified by the bisection method. It is the x-coordinate, where the Taylor series exceeds the user-defined error of the linear approximation starting at the previous point, and ε is the user-defined value of this error. The aim is to reject a solution which would be beyond the neighborhood zone. When a solution with a certain time step at a certain node falls beyond the neighborhood zone, it is rejected, the time step is decreased, and a new solution is evaluated. If the solution falls into the same zone as that of the previous time step, the time step is increased. If the solution falls into the neighborhood zone, the solution is still accepted, and the time step is unchanged. Thus we can make the generalization that the length of the time step is dependent on the retention curve torsion.

3.3. Case study

A case study was conducted in order to evaluate numerical solution to the classical Richards' equation model. Three different approaches were tested. Solution based on *mixed*-form a so called Modified Picard Iteration, see (6), solution based on h-based form (2) with time step restriction as defined here as the Retention Curve Zone Approach, and a solution of h-based form (2) without Retention Curve Zone Approach restrictions to the time step—this is exactly the form that is not recommended in [3]. An adaptive time discretization for the last method was considered as for the *mixed*-form equation (the iteration criterion).

The criterion of successful iteration for all of the three evaluated methods was a minimal relative change of a pressure head h lower then 10^{-4} from the previous iteration level.

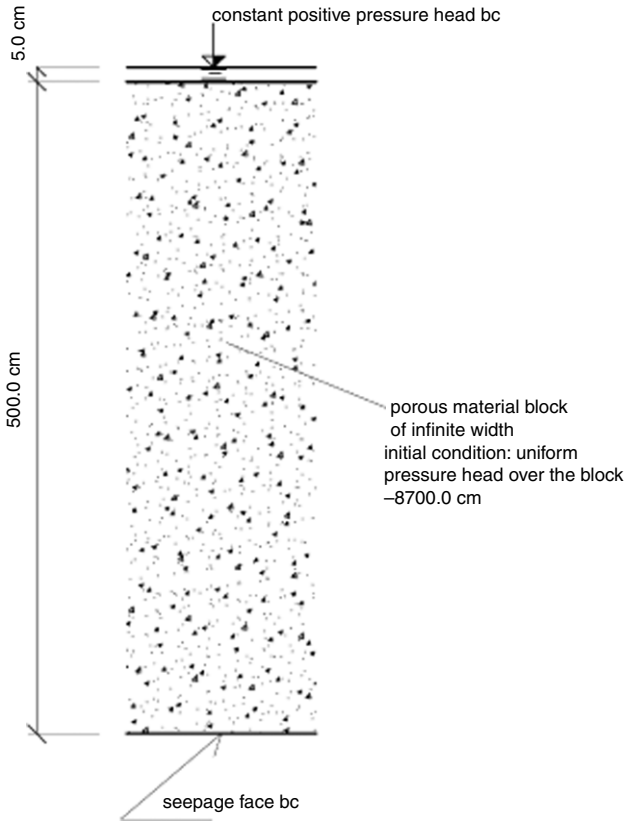

Fig. 2. Scheme of the one-dimensional vertical infiltration experiment.

3.3.1. Description of the case study

A simulation of a vertical one-dimensional infiltration experiment was conducted, see Fig. 2. The flow experiment was described by the classical Richards' equation. The selected flow domain was a porous material block 5 m in length and of infinite width. Thus only vertical one-dimensional flow was taking place. Porous material properties was considered for highly permeable sandstone ($\alpha = 0.075\ \mathrm{cm}^{-1}$, $n = 1.89$, $m = 0.47$, $K_s = 4.42\ \mathrm{cm\ h}^{-1}$). The maximal error of a first-order Taylor series for the Retention Curve Zone Approach was 5×10^{-6}.

The domain was discretized by an uniform mesh of grid size 5 cm.

The problem was solved numerically using three different approaches as stated above.

3.3.2. Boundary and initial conditions

The initial condition was uniform distribution of the water content, represented by a negative pressure head ($h = -8700$ cm), for the relation between the negative pressure head and the water content see (5).

The top boundary condition was the standard Dirichlet condition of a positive constant pressure head $+5.0$ cm.

The bottom boundary condition was of a special kind. Technically, it is called a seepage face. Physically this condition states that if the boundary is unsaturated it acts as a no-flow boundary, and when it is saturated it acts as a Dirichlet boundary of a zero pressure head. Mathematically, it is defined as a unilateral boundary condition, a combination of the Dirichlet condition and the Neumann condition. The following form describes the condition

$$\begin{aligned} &\frac{\partial h}{\partial \vec{n}}(x,t) + \nu_3(x) = 0, \quad \text{if } h(x,t) < 0,\ \forall x \in \Gamma, t > 0 \\ &h(x,t) = 0, \quad \text{if } \frac{\partial h}{\partial \vec{n}}(x,t) + \nu_3(x) < 0,\ \forall x \in \Gamma, t > 0 \end{aligned} \tag{9}$$

where $\vec{n}$ is the direction of the normal vector to the domain boundary, ν_3 is the vertical component of the normal vector to the domain boundary, and Γ is the boundary where this condition applies.

3.4. Results and discussion

As stated in [3] the successful iteration criterion for an adaptive time step of the Eq. (2) is not a sufficient condition to ensure a certain accuracy if the time derivative term is handled by the implicit backward Euler method. The Modified Picard

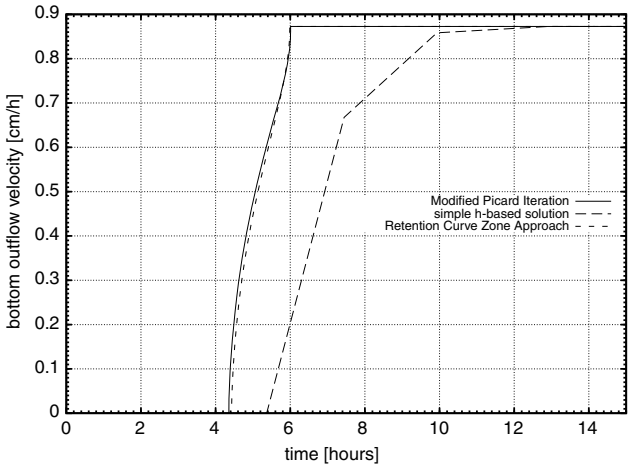

Fig. 3. Simulated outflow from a seepage face with the DRUtES algorithm. The Retention Curve Zone Approach, Modified Picard Iteration and time step based on successful iteration of (2) were tested.

Table 1
Summary of code execution after the numerical infiltration experiment.

Method	Mass error (%)	Number of iterations
Retention Curve Zone Approach	0.193	1746
Modified Picard Iteration (6)	0.201	44 382
Simple *h*-based solution (2)	5.842	130

Iteration method obtains very accurate results, but the computational effort in the evaluated case is excessive. The Retention Curve Zone Approach obtains practically the same results, but the total amount of iteration is only approximately 4% of the amount required for the Modified Picard Iteration method.

This method offers an efficient condition for a numerical solution to a *h*-based equation based on an implicit backward Euler scheme, exactly reflecting the problem of the approximation (8).

Although the problem with the mass balance of (2) would be easily solvable by applying of (3), the definition scope of this equation is restricted to a negative pressure head, and thus it is not suitable for the case study evaluated here.

For the particular results see Table 1 and Fig. 3.

4. Mathematical model of the dual porosity conceptual approach

This section presents an extension to the classical Richards' equation model, suitable for porous materials with distinctive preferential flow paths like fractures, fissures, etc.

The dual porosity conceptual model is based on some assumptions—the medium is separated into two distinct pore systems, each of which is treated as a homogeneous medium with separate hydraulic properties. The dual porosity medium is considered to be a superposition of these two systems over the same volume [19]. Darcian type flow is considered both for the fractures and for the matrix pore system, while the transfer of water is described macroscopically using a first-order coupling term [8].

The original approaches lead to a system of coupled nonlinear partial differential equations. If the parameters are correctly maintained, there are significant simplifications in mesh structure and in the resulting system of linear equations compared with direct microscopic fracture flow modeling.

4.1. Governing equations

The governing equation for Darcian water flow in a variably saturated rigid dual porosity medium, under the assumptions that the pressure is constant in the air phase and the fluid is incompressible, is stated as [8]

$$\begin{aligned} C(h_m)\frac{\partial h_m}{\partial t} &= \nabla.\left(K_m(h_m)\nabla h_m\right) + \frac{\partial K_m(h_m)}{\partial z} + \alpha\frac{(h_f - h_m)}{1-\omega_f} - S_m \\ C(h_f)\frac{\partial h_f}{\partial t} &= \nabla.\left(K_f(h_f)\nabla h_f\right) + \frac{\partial K_f(h_f)}{\partial z} - \alpha\frac{(h_f - h_m)}{\omega_f} - S_f \end{aligned} \tag{10}$$

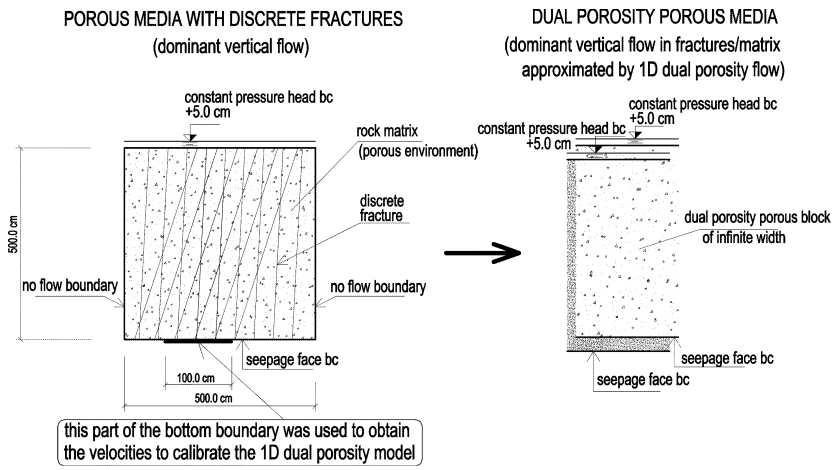

Fig. 4. Scheme of the case study for a dual porosity model.

where subscripts f and m denote the subsystem of fractures (macropores) and matrix blocks (micropores), ω is a volume fraction [–], S is a sink term [T^{-1}], α_w is the first-order mass transfer coefficient [$L^{-1}.T^{-1}$]. This coefficient was presumed in [20] to be of the form

$$\alpha_w = \frac{\beta}{\alpha^2} K_a \gamma_w \tag{11}$$

where β is a dimensionless geometry coefficient, α is the characteristic half width [L] of the matrix block, K_a is the effective hydraulic conductivity [$L.T^{-1}$] of the matrix at or near the fracture/matrix interface, and γ_w is a dimensionless scaling factor.

5. Numerical solution of the dual porosity Richards' equation model

The numerical solution to the conceptual model presented in the previous chapter, the dual porosity Richards' equation model (10) is retained in this section. The method is based on the technique presented as the Retention Curve Zone Approach in Section 3.2.1. Thus the h-based form (10) is solved by the fully implicit backward Euler scheme with a time step restriction based on the retention curve torsion. In this case the zone check is performed for the retention curves of the matrix and of the fracture domain.

Two different approaches to a numerical solution to (10) were already distinguished in [8]. The both equations might be solved consecutively by applying an iterative scheme to estimate and update the unknown pressure head vector of the second pore system, or they might be solved simultaneously. The latter option leads to matrices that are twice as large as the matrices with the first option, and with some extra bands depending on the problem dimension, but as mentioned in [8] it provides more stable behavior. In [11], Tseng et al. maintain some domain decomposition techniques to simplify the matrices by splitting the fracture and the matrix flow domain, but some restrictions in stability are also observed.

The numerical solver presented here was built on a simultaneous solution to the both equations in (10). The unsaturated hydraulic conductivity function in (11) was defined by the unsaturated hydraulic properties of the matrix domain, and the pressure head for evaluating this value was assumed to be an average value to the pressure head in both the matrix and fracture domains. The ratio $\gamma_w \frac{\beta}{\alpha^2}$ was considered to be a user definable value, as these coefficients are constant material parameters.

5.1. Case study

This case study evaluates the dual porosity model, which was performed as a calibration of this homogeneous approach to an infiltration experiment on a rock sample with discrete fractures, see Fig. 4.

5.1.1. Infiltration experiment on a rock sample with discrete fractures

This experiment was conducted on a sample with discrete fractures. The construction of this discrete matrix/fracture model was model is dealt with in [21], and will therefore be discussed only very briefly here. This fracture model was constructed in order to conduct an experiment to obtain data for calibrating the dual porosity model. The aim was to homogenize a rock environment with seismic fractures in the neighborhood to one of the recent major nuclear waste repository in Czech Republic, Richard–Litoměřice. This model was based on a geostatistic study published in [22].

Fig. 4 explains the infiltration experiment. Highly conductive fracture path-lines over a low conductive rock matrix were assumed. A cross flow between matrix and fractures was also assumed. Fracture flow has been defined by the

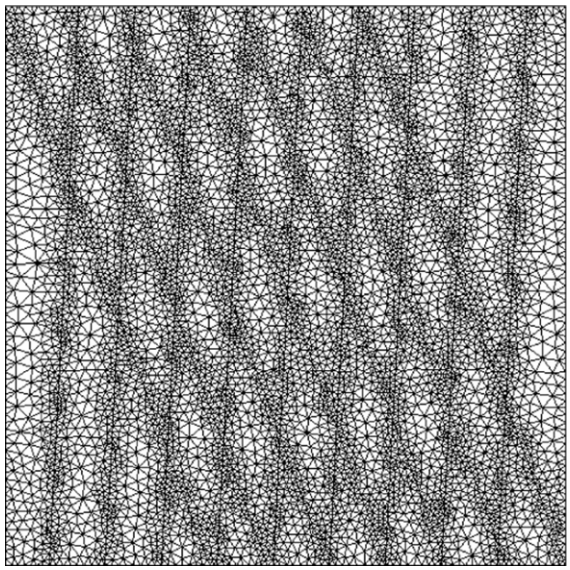

Fig. 5. Mesh discretization of the domain of the infiltration experiment on the discrete fracture rock sample.

Table 2
Rock matrix properties obtained from [22].

θ_r [–]	θ_s [–]	α [cm^{-1}]	n [–]	m [–]	K_s [cm^{-1} d^{-1}]
0.064	0.14	0.01	2.5	0.6	0.0864

Hagen–Poiseuille law (the fracture width was assumed 0.05 mm), and the flow in the rock matrix is defined by a classical Richards' equation. The experiment was conducted using the commercially-available FEFLOW code [23]. This discrete fracture model was approximated by a mesh of 13 595 elements and 6963 nodes with its higher density in the vicinity of the fracture, see Fig. 5. For a detailed description of the numerics of this experiment see [21,23]. A more detailed description is beyond the scope of this paper.

Boundary and initial conditions. The initial condition was assumed to be 60% saturation of the equivalent water content θ_E, where $\theta_E = \frac{\theta_S - \theta}{\theta_S - \theta_r}$, for the matrix pore system, and zero saturation for the fractures.

Both vertical boundaries were assumed to be of a Neumann kind—no flow. The top horizontal boundary was of a Dirichlet kind—a constant pressure head, and the bottom boundary was an unilateral kind —seepage face, see (9), a combination of a Neumann boundary condition type and a Dirichlet boundary condition type.

5.1.2. Dual porosity flow approximation

A dual porosity model was constructed to approximate the flow on the model introduced in Section 5.1.1. This approximation will be used in some future studies of the Richard nuclear waste repository. As the flow on the two-dimensional discrete fracture/matrix model is predominantly vertical, a one-dimensional dual porosity model was assumed to give an accurate approximation of the experiment introduced in Section 5.1.1.

The unsaturated hydraulic properties of the matrix in the dual porosity model were given by the rock matrix of the discrete fractures/matrix rock sample, see Table 2.

The unsaturated hydraulic properties of the fast fracture domain in the dual porosity model (10) were identified by a parameter identification procedure.

The aim of the dual porosity approximation was to obtain an identical bottom outflow fluxes and volumes for an infiltration experiment identical to that conducted on the discrete fractures/matrix model in Section 5.1.1.

In order to obtain the worst possible scenario (the most conductive fractured material), only the part of the boundary with the highest fracture density as shown in Fig. 4 was assumed for calibrating the dual porosity model.

The domain was discretized by a uniform mesh of 5 cm grid size.

Boundary and initial conditions. The initial condition for the matrix domain was 60% saturation of the equivalent water content θ_E, where $\theta_E = \frac{\theta_S - \theta}{\theta_S - \theta_r}$ for the matrix pore system, and zero saturation for the fracture domain (θ_r for the fracture domain was assumed to be zero, as stated in [8]).

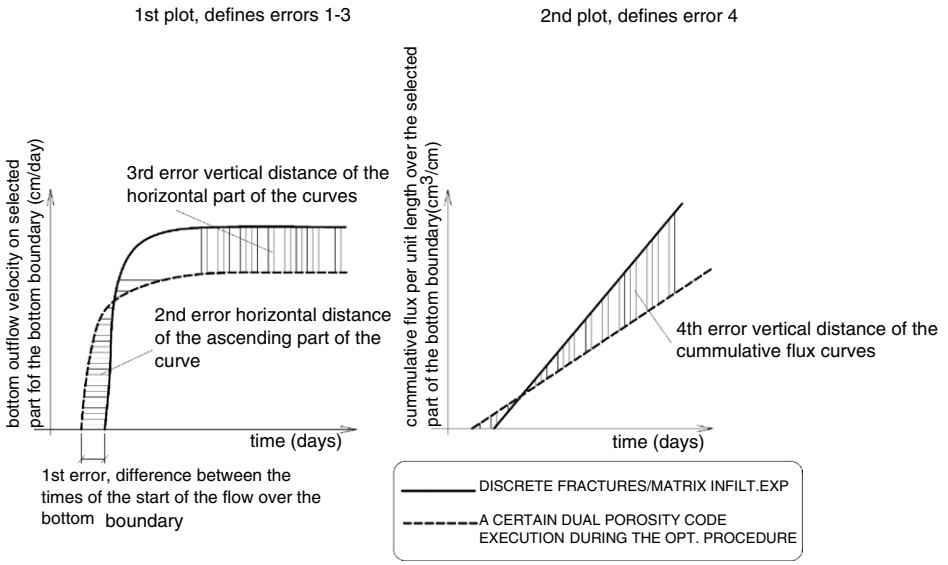

Fig. 6. Scheme of the optimization procedure, error 1 only emphasizes error 2 at the beginning of the flow.

The boundary condition was identical for the fracture domain and for the matrix domain. The top boundary was a Dirichlet condition of a constant positive pressure head +5.0 cm, the bottom boundary condition was a seepage face (9).

5.2. Optimization procedure

The parameters to be calibrated are the unsaturated hydraulic parameters of the fast domain (van Genuchten's retention curve parameters (5) – α, n, m; porosity (saturated water content) – θ_s, saturated hydraulic conductivity K_S), the ratio $\gamma_w \frac{\beta}{\alpha^2}$ from Eq. (11) and the fast domain ratio ω_f from Eq. (10), a total of seven parameters. The residual water content θ_r was assumed to be zero, as stated in [8].

The function to be optimized is highly nonlinear and non-convex. The problem of the global extremes of non-convex functions has still not been satisfactorily solved. A genetic algorithm application was therefore used to provide a solution that is considered technically suitable.

An evolutionary algorithm was applied, based on SADE [24] and enhanced by the multi-objective selection mechanism known as Average Ranking (AR) [25,26].

The problem of identifying the input parameters is generally an inverse task, where some unknown inputs of a model are searched to obtain required, a priori given outputs. We follow the forward mode of an inverse analysis [27], which minimizes the error function defined as the difference between the measured data and the responses obtained from the model. Since the computational demands of a single simulation of the problem are low, direct search methods can be applied. These usually need more computational resources but do not require any gradient information. Hence, the only difficulty within the forward mode is to make a proper selection of the error function. One option is to choose a single global error function but this is usually multi-modal and ill-posed. It is therefore recommended to select several error functions. It is easy to incorporate both expert knowledge and preferences for the importance of different parts from among the results, as will be shown below. Moreover, this methodology permits us intuitively to include further criteria, e.g. monotonicity or minimum curvature conditions.

By selecting four error functions we have tried to obtain as realistic an output as possible and also to help the optimization algorithm during the search to find a Pareto set quickly. All four errors aim at specific physical phenomena during the flow, namely the beginning of the flow through the bottom boundary. As the unilateral boundary condition, technically identified as the seepage face boundary condition, was used. The start of the flow can therefore be described as the switch between Neumann's no-flow boundary and Dirichlet's zero pressure head boundary, see Eq. (9) in Section 3.3.2. The next two errors were identified as the steep middle part of the graph of fluxes and the final steady state flux. This is important for obtaining an identical macroscopic velocities of this approximation, which is crucial for contaminant transport modeling. Finally the fourth error was assumed to be an error in the flux cumulation per unit length curve, in order to place the emphasis of the optimization algorithm on the mass, a very important phenomenon in this conceptual approximation to the discrete fracture model.

The volume cumulation was related to a unit length of the part of the bottom boundary as seen on Fig. 4 due to the one-dimensional dual porosity code.

The first three functions were tested on a graph of velocities on the bottom boundary and the time of the experiment, while the fourth error was tested on a graph of the cumulation of the boundary flux volume per unit length in time.

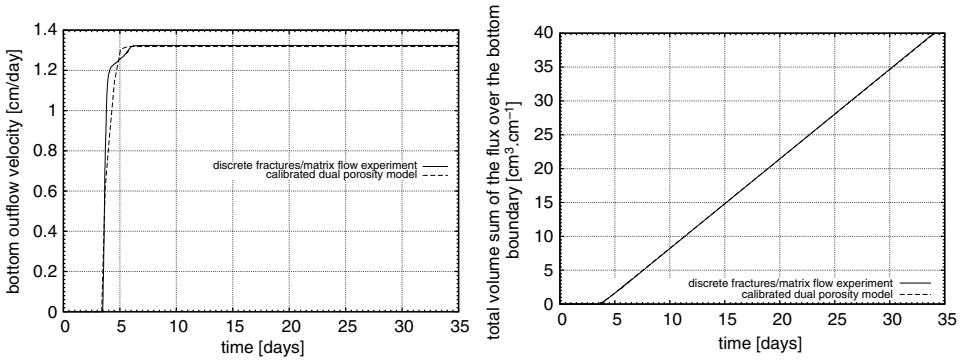

Fig. 7. Left: Plot of the fluxes over the bottom boundary of the discrete fractures/matrix flow model and the calibrated dual porosity model. Right: Plot of the sum of the fluxes over the bottom boundary of the discrete fractures/matrix flow model and the calibrated dual porosity model, due to a successful calibration both lines are merged in this plot.

Table 3
The ranges of the parameters of the fast domain processed in optimization procedure and its identified values.

Parameter type	High range	Low range	Identified value
Ret. curve par.: α [cm^{-1}]	10^{-2}	10^{-3}	0.00682589
Ret. curve par.: n [–]	6.0	1.5	5.48293
Ret. curve par.: m [–]	0.7	0.1	0.433692
Porosity: θ_s [–]	1.0	10^{-4}	0.910872
Sat. hydr. conduct.: K_s [cm.d^{-1}]	2.785×10^4	1.0	15.9464
Term from Eq. (11): $\gamma_w \frac{\beta}{\alpha^2}$ [cm^{-2}]	10.0	0.0	8.89911
Fast domain ratio from Eq. (10): ω_f [–]	0.75	1×10^{-4}	0.0292884

The first error function is the squared difference between the times of the starts of flows from both simulations. The second function is the horizontal RMS error in terms of the ascending part of the graph. The third function was the vertical RSM error which is intended to achieve the same level of maximal flux and finally there is the vertical RMS error on the curve of the cumulative fluxes, for details see Fig. 6.

5.3. Results and discussion

The optimization algorithm executed the dual porosity code a total of 1×10^6 times, but the steepest descending part of the error function was only up to 1×10^5 executions, and the rest of the code runs led only to minor decrements in the evaluated error function.

By inspecting all visited solutions during the search and also the obtained Pareto front, a dozen solutions can be found with a zero first error, an error representing the start of the flow over the bottom boundary, thus the switch in the condition (9).

As shown on Fig. 7, the velocity curve of the calibrated model suffered from a minor error in the steeply ascending part, thus in the second error, which is of the lowest importance among all the evaluated errors. The third error, represented by the maximal flux, had again a zero value. The fourth error, representing the volume cumulation of the bottom boundary flux was so low, that the plot of the curve out of the discrete fracture/matrix model and the curve of the calibrated dual porosity model are merged.

Based on the results of the dual porosity code presented here, the calibration was successful, see Table 3 for the identified unsaturated hydraulic parameters of (10). As shown on Fig. 7, the dual porosity approximation is almost identical to the discrete fracture/matrix model, mainly the volume cumulation. This only in fact demonstrates what has already been stated in several fundamental works [8,17,19].

6. Conclusions

This paper has presented a numerical solution both for the classical Richards' equation [1] and for Richards' equation with a dual porosity conceptual model [8].

A new technique, defined here as the Retention Curve Zone Approach for maintaining an adaptive step, has been designed and tested here. Its suitability for a numerical solution of the h-based Richards' equation has been presented on the basis of a numerical one-dimensional vertical infiltration experiment. This technique is based on reflecting the error in the linear approximation of the time derivative term (8). This method has been evaluated against two different approaches, against an iterative solution to the mixed form of Richards' equation (1) and a solution to the h-based Richards' equation (2) without the

application of the Retention Curve Zone Approach technique. The *h*-based solution with the Retention Curve Zone Approach technique and the *mixed*-based solution offered almost identical results, but the former required lower computational effort, due to its faster convergence. The numerical solution without the Retention Curve Zone Approach technique suffered with mass conservation problems exactly as stated in [3].

Based on those results the Retention Curve Zone technique was also applied for Richards' equation solver in the dual porosity conceptual model [8]. A numerical solution was evaluated on calibration against data obtained from a numerical simulation on a rock sample with discrete fractures—preferential paths. A very accurate fit was observed in terms of mass and macroscopic velocities compared to the discrete model. The results will be used in future studies evaluating the contaminant transport from the Richard nuclear waste repository at Litoměřice, Czech Republic.

The DRUtES computer program has been released under an ordinary GNU/GPL license as a result of this work. Its source code is available from the public GNU community web sites.

Acknowledgements

Financial support from the Ministry of Agriculture of the Czech Republic (research project NAZV EC – 91247) and from the Czech Ministry of Education (research projects MSM 6840770003 and MSM 0021620855) is gratefully acknowledged.

References

[1] L.A. Richards, Physics 1 (1931) 318–333 doi:10.1063/1.1745010.
[2] H.W. Alt, S. Luckhaus, Quasilinear elliptic–parabolic differential equations, Mathematische Zeitschrift 183 (1983) 311–341.
[3] M.A. Celia, E.T. Bouloutas, R.L. Zarba, A general mass-conservative numerical solution for the unsaturated flow equation, Water Resources Research 26 (1990) 1483–1496.
[4] J. Kačur, Solution of degenerate convection-diffusion problems, Nonlinear Analysis 47 (2001) 123–134.
[5] J. Kačur, R. van Keer, Numerical approximation of a flow and transport system in unasaturated-saturated porous media, Chemical Engineering Science 58 (2003) 4805–4813.
[6] G.I. Barenblatt, I.P. Zheltov, Fundamental equations of filtration of homogeneous liquids in fissured rocks, Doklady Akademii Nauk SSSR 13 (1960) 545–548.
[7] G.I. Barenblatt, I.P. Zheltov, I.N. Kochina, Basic concepts in the theory of seepage of homogeneous liquids in fissured rocks, Journal of Applied Mathematical Mechanics 24 (1960) 1286–1303.
[8] H.H. Gerke, M.T. van Genuchten, A dual-porosity model for simulating the preferential movement of water and solutes in structured porous media, Water Resources Research 29 (1993) 305–319.
[9] M. Larsbo, S. Roulier, F. Stenemo, R. Kasteel, N. Jarvis, An improved dual permeability model of water flow and solute transport in the vadose zone, Vadose Zone Journal 4 (2005) 398–406.
[10] P.F. Germann, Kinematic wave approach to infiltration and drainage into and from soil macropores, Transactions on ASAE 28 (1985) 745–749.
[11] P.H. Tseng, A. Scortino, M.Th. van Genuchten, A partitioned solution procedure for simulating water flow in a variably saturated dual porosity medium, Advances in Water Resources 18 (1995) 335–343.
[12] J.B. Kool, J.C. Parker, M.Th van Genuchten, Parameter estimation for unsaturated flow and transport models—A review, Journal of Hydrology 91 (1987) 255–293.
[13] T. Wöhling, J.A. Vrugt, G.F. Barkle, Comparison of three multiobjective optimization algorithms for inverse modeling of vadose zone hydraulic properties, Soil Sciency Society of America Journal 75 (2008) 305–319.
[14] J. Bear, A. Veruijt, Modeling Groundwater Flow and Pollution, D. Reidel Publishing Company, New York, 1987.
[15] Y. Mualem, A new model for predicting the hydraulic conductivity of unsaturated porous media, Water Resources Research 12 (1976) 513–522.
[16] M.T.H. van Genuchten, Calculating the Unsaturated Hydraulic Conductivity with a New, Closed Form Analytical Model, Research Report 78-WR-08, Water Resources Program, Department of Civil Engineering, Princeton University, Princeton, 1978.
[17] M.T.H. van Genuchten, A closed-form equation for predicting the hydraulic conductivity of unsaturated soils, Journal of Soil Science 44 (5) (1980) 892–898.
[18] Rank Ernst, Katz Casimir, Werner Heinrich, On the importance of the discrete maximum principle in transient analysis using finite element methods, International Journal for Numerical Methods in Engineering 19 (1983) 1771–1782.
[19] R.C. Dykhuizen, Transport of solutes through unsaturated fractured media, Water Research 21 (1987) 1531–1539.
[20] H.H. Gerke, M.T. van Genuchten, Evaluation of the first order transfer term for variably saturated dual porosity flow models, Water Resources Research 29 (1993) 1225–1238.
[21] M. Kuráž, D. Trpkošová, Estimating dual permeability parameters of the fractured environment of the richard nuclear repository, in: International Conference on the Practical Aspects of Deep Geological Disposal of Radioactive Waste, 2008.
[22] L. Vrbata, J. Činka, A Hydrogeological and geotechnical monitoring of storage facility richard and bratrtsvi in 2005, Geotip technical report, RAWRA, 2005.
[23] H.-J.G. Diersch, White Papers Volume I., WASY Software FEFLOW 5.2, Berlin, 2005.
[24] O. Hrstka, A. Kučerová, Improvements of real coded genetic algorithms based on differential operators preventing the premature convergence, Advances in Engineering Software 35 (2004).
[25] P.J. Bentley, J.P. Wakefield, An analysis of multiobjective optimization within genetic algorithms, Technical Report ENGPJB96, University of Huddersfield, UK, 1996.
[26] M. Lepš, Parallel multi-objective identification of material parameters for concrete, in: Proceedings of the Ninth International Conference on the Application of Artificial Intelligence to Civil, Structural and Environmental Engineering, Stirling: Civil-Comp Press Ltd, 2007.
[27] A. Kučerová, Identification of nonlinear mechanical model parameters based on soft computing methods, Ph.D. Thesis, Ecole Normale Supérieure de CACHAN (27/11/2007), http://tel.archives-ouvertes.fr/tel-00256025/fr/.